Europium-containing ionic liquids and crystal complexes based on phosphine oxides

Haiwang Liu [1], Chuandong Deng [1], Qingde Chen, Xinghai Shen *

Beijing National Laboratory for Molecular Sciences (BNLMS), Fundamental Science on Radiochemistry and Radiation Chemistry Laboratory, College of Chemistry and Molecular Engineering, Peking University, Beijing 100871, PR China

ABSTRACT

We synthesized two Eu-containing ionic liquids (ILs) $[Eu(TOPO)_4(NO_3)_2]NTf_2$ and $[Eu(TBPO)_4(NO_3)_2]NTf_2$, and a crystal $[Eu(TPhPO)_4(NO_3)_2]NTf_2$. In these complexes, TOPO (Tri-*n*-octylphosphine oxide) and TBPO (Tri-*n*-butylphosphine oxide) coordinate with Eu^{3+} constituting the cations, while NTf_2^- (bis(trifluoromethylsulfonyl)imide anion) acts as the counter anion. The crystal structure of $[Eu(TPhPO)_4(NO_3)_2]NTf_2$ showed the details of the coordinated condition. The infrared spectra of all the complexes exhibited some typical features of the phosphine oxides and two bidentate nitrates. $[Eu(TRPO)_4(NO_3)_2]^+$ (R = octyl and butyl) were proved to exist in the $C_2H_2Cl_2$ solutions by ^{31}P NMR of $[Eu(TOPO)_4(NO_3)_2]NTf_2$ and $[Eu(TBPO)_4(NO_3)_2]NTf_2$. The luminescence emissions also gave information about the same coordination environments. Thermogravimetric analyses (TGA) indicated that the NTf_2^- group determined the decomposition temperatures of the three complexes. These complexes are the first tetra-phosphine oxide complexes constituted by $Eu(NO_3)_3$ and phosphine oxides in the presence of NTf_2^-. The structural difference between $[Eu(TRPO)_4(NO_3)_2]NTf_2$ in this work and $Eu(TRPO)_3(NO_3)_3$ formed in traditional organic solvent can help understand that new extraction species may exist in the NTf_2^--based IL extraction system different from those in the normal organic solvent extraction system.

© 2016 Elsevier Ltd. All rights reserved.

1. Introduction

Phosphine oxides and their complexes with lanthanide nitrates have been investigated widely in the separation and solvent extraction of lanthanides. The association of TOPO and TBPO with lanthanide nitrates usually leads to the formation of the complexes $Ln(TOPO)_3(NO_3)_3$ and $Ln(TBPO)_3(NO_3)_3$, respectively [1,2]. In the extraction of Am and Cm, the extracted complexes were deduced to be $Am(TOPO)_3(NO_3)_3$, $Am(TBPO)_3(NO_3)_3$, $Cm(TOPO)_3(NO_3)_3$ and $Cm(TBPO)_3(NO_3)_3$ [3]. The reactions of TPhPO (Triphenylphosphine oxide) with lanthanide nitrates in ethanol and acetone produced $Ln(TPhPO)_3(NO_3)_3$, in which nine-coordinate metal centres based on three bidentate nitrates and three phosphine oxides were revealed [4,5]. Levason et al. [6] reported a detailed study of the reaction of a large excess of TPhPO with lanthanide nitrates. They found that nine-coordinate $Ln(TPhPO)_4(\eta^2-NO_3)_2(\eta^1-NO_3)$ for the light lanthanide (La, Ce, Pr, Nd) ions and eight-coordinate $[Ln(TPhPO)_4(\eta^2-NO_3)_2]NO_3$ for the heavy lanthanide (Ho, Yb, Lu) ions were formed, whereas only nine-coordinate $Ln(TPhPO)_3(\eta^2-NO_3)_3$

was formed under similar conditions for the middle lanthanide (Sm, Eu, Gd) ions. Recently, Bowden et al. [7] examined the formation of TRPO (Trialkylphosphine oxide) with varying steric demands with lanthanide nitrates and studied their properties. For the lighter lanthanide (Ce, Pr, Nd, Eu) ions, complexes $Ln(TEtPO)_3(NO_3)_3$ were formed, while $Ln(TEtPO)_3(NO_3)_3$ and $Ln(TEtPO)_2(NO_3)_3$ were formed for the heavier lanthanide (Tb and Ho) ions. With the increasing size of the ligand, $Ln(TRPO)_3(NO_3)_3$ (R = cyclohexyl [8] and isobutyl [9]) were formed throughout the lanthanide series and some subtle variations in structure appear as the ionic radius decreases. When the ligand is bulky T^tBuPO (Tri-tertbutylphosphine oxide), complexes of $Ln(T^tBuPO)_2(NO_3)_3$ were formed for all lanthanides instead of $Ln(T^tBuPO)_3(NO_3)_3$ [10]. The summary of these complexes was listed in Table 1.

Ionic liquid (IL) attracts much attention in many fields including catalysis, synthesis and solvent extraction [11–13]. In solvent extraction, ionic liquid has been considered as an alternative solvent due to its unique properties such as low vapor pressure, high stability and solvating properties [13–22], while some organic solvents are usually flammable, volatile, and toxic. In addition, the physicochemical properties (such as polarity, immiscibility, and viscosity) of ILs are effectively tunable, depending on the alternative cations and anions [23]. Now, the most widely used IL is

---

* Corresponding author. Tel.: +86 10 62765915; fax: +86 10 62759191.
 E-mail address: xshen@pku.edu.cn (X. Shen).
 [1] The first two authors contributed equally to this paper.

Table 1
Complexes formed on reaction of lanthanide nitrates and TPhPO or other TRPOs in references [6–10].

Lanthanides	TPhPO		TEtPO	TRPO (R = cyclohexyl and isobutyl)	TRPO (R = tert butyl)
	TPhPO:Ln < 4 (molar ratio)	TPhPO:Ln > 6 (molar ratio)			
Light lanthanides (La, Ce, Pr, Nd)	Ln(TPhPO)$_3$(NO$_3$)$_3$ (nine-coordinate)	Ln(TPhPO)$_4$(NO$_3$)$_3$ (ten-coordinate)	Ln(TEtPO)$_3$(NO$_3$)$_3$ (nine-coordinate)	Ln(TRPO)$_3$(NO$_3$)$_3$ (nine-coordinate)	Ln(T^{t}BuPO)$_2$(NO$_3$)$_3$·H$_2$O·EtOH (nine-coordinate)
Middle lanthanides (Sm, Eu, Gd)	Ln(TPhPO)$_3$(NO$_3$)$_3$ (nine-coordinate)	Ln(TPhPO)$_3$(NO$_3$)$_3$ (nine-coordinate)	Ln(TEtPO)$_3$(NO$_3$)$_3$ (nine-coordinate)	Ln(TRPO)$_3$(NO$_3$)$_3$ (nine-coordinate)	Ln(T^{t}BuPO)$_2$(NO$_3$)$_3$·EtOH (eight-coordinate)
Heavy lanthanides (Ho, Yb, Lu)	Ln(TPhPO)$_3$(NO$_3$)$_3$ (nine-coordinate)	Ln(TPhPO)$_4$(NO$_3$)$_3$ (eight-coordinate)	Ln(TEtPO)$_3$(NO$_3$)$_3$ (nine-coordinate) and Ln(TEtPO)$_2$(NO$_3$)$_3$ (eight-coordinate)	Ln(TRPO)$_3$(NO$_3$)$_3$ (nine-coordinate)	Ln(T^{t}BuPO)$_2$(NO$_3$)$_3$ (eight-coordinate)

$C_n$mimNTf$_2$ (1-alkyl-3-methylimidazolium bis(trifluoromethylsulfonyl)imide) in solvent extraction because of their low viscosity (the structure of NTf$_2^-$ is shown in Scheme 1). The challenge for developing the practical applications of ILs in metal ion separation is to understand the different coordination modes in ILs, which may lead to a much higher extraction efficiency. As known, TRPO are traditional extractants with high extraction efficiency on lanthanides. In traditional solvent extraction, extensive studies on lanthanide complexes revealed that Ln(TRPO)$_3$(NO$_3$)$_3$ are often formed [1,2]. But in the IL-extraction system, because the extraction mechanism is often different, we have to take the influence of added ILs on the extraction complexes into consideration. Especially, the influence of NTf$_2^-$ on the structure of complexes needs to be studied, as most extraction mechanism of neutral extractants in ILs is a cation-exchange mechanism [14,18,22,24,25].

Herein, we report the synthesis and characterization of the complexes of Eu(NO$_3$)$_3$, TOPO (or TBPO, TPhPO) with NTf$_2^-$ in order to understand the structural characteristics and physico-chemical properties of the Europium-containing ionic liquids and crystal complexes based on phosphine oxides. The structures of the ionic liquid $C_n$mimNTf$_2$ and the phosphine oxides used in this work are shown in Scheme 1.

2. Experimental

2.1. Materials

C$_4$mimNTf$_2$ was synthesized via metathetical reaction between C$_4$mimBr and LiNTf$_2$ [26]. Both C$_4$mimBr and LiNTf$_2$ were purchased from Lanzhou Institute of Chemical Physic, Chinese Academy of Sciences. TOPO (Aldrich), TBPO (Acros), TPhPO (TCI) and Eu(NO$_3$)$_3$·6H$_2$O (China Minmetals Research Institute) were of analytical grade and used without further purification. C$_2$H$_5$OH, CH$_2$Cl$_2$ and CH$_3$CN were purchased from Beijing Chemical Reagents Co. and were of analytical grade. Tridistilled water was used throughout the experiments.

2.2. Instruments

The high-resolution mass spectrometry used with electrospray ionization (ESI-HRMS) was done on a Fourier transform ion cyclotron resonance mass spectrometer, APEX IV (Bruker, USA). The organic element analysis was performed on an elemental analyzer, vario EL (Elementar Analysensysteme GmbH, Germany). FTIR spectra of the complexes were recorded on a NICOLET iN10 MX spectrometer using the infrared microspectroscopy method. The thermogravimetric analyses (TGA) were measured on a Q600 SDT thermoanalyzer under N$_2$ atmosphere with the temperature ranging from 25 to 1000 °C at a heating rate of 5 °C min^{-1}. The melting point was measured by the melting point detector. The ^{31}P NMR spectra were recorded on a 600 MHz Varian VNMRS spectrometer with a 5 mm broadband probe. The crystallographic data for the single crystal were collected on an Agilent SuperNova Dual Atlas CCD diffractometer. Monochromated Mo Kα (λ = 0.71073 Å) radiation was used. Using OLEX2, the structure was solved with the XS structure solution program using direct methods and refined with the XL refinement package using least squares minimization. The hydrogen atoms were added according to the ideal geometry, and were not refined for good refinement convergence.

2.3. Preparation

A 20 mL of ethanol solution containing both an extractant (TOPO, TBPO or TPhPO) (0.2 mol·dm^{-3}) and LiNTf$_2$ (0.2 mol·dm^{-3}) was heated to 60 °C. The solution was stirred continuously until it
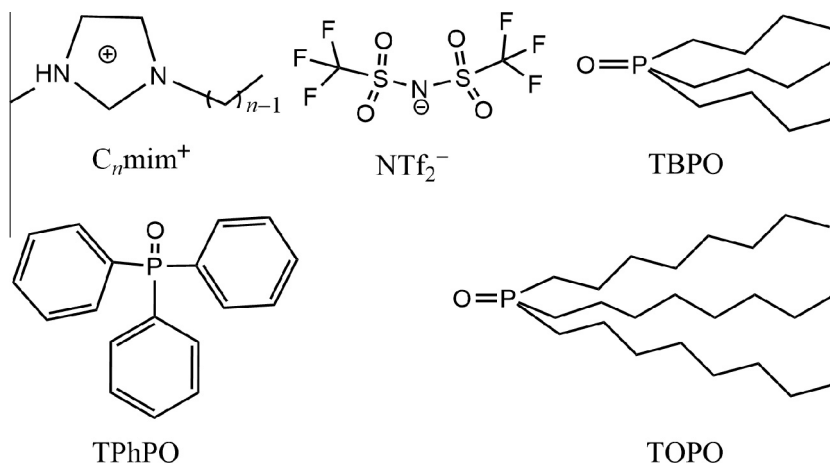
Scheme 1. The structures of the ionic liquid $C_n$mimNTf$_2$ and the phosphine oxides used in this work.

became clear. Then a 10 mL aqueous solution of Eu(NO$_3$)$_3$ (0.5 mol·dm^{-3}) was added dropwise into the above ethanol solution. The mixed solution was stirred continuously for 4 h at 60 °C and was then cooled down slowly. Clear viscous liquids or white solid product were obtained, depending on which extractant was used.

For TOPO and TBPO, colorless liquids were gotten from the bottom of the flask and washed with water in order to remove the un-reacted LiNTf$_2$ and Eu(NO$_3$)$_3$. The liquids were further purified by mixed solvent (ethanol and water) to remove the possible impurities (TOPO or TBPO). The viscous liquids were washed several times by the above mixed solvent until they were completely purified. The purified liquid products were characterized by ESI-HRMS and organic element analyses and were proved to be [Eu(TOPO)$_4$(NO$_3$)$_2$]NTf$_2$ and [Eu(TBPO)$_4$(NO$_3$)$_2$]NTf$_2$. The results of organic element analyses were consistent with the calculated values. The yield for [Eu(TOPO)$_4$(NO$_3$)$_2$]NTf$_2$ is 76%. *Anal.* Calc. (found) for [Eu(TOPO)$_4$(NO$_3$)$_2$]NTf$_2$ (C$_{98}$H$_{204}$EuF$_6$N$_3$O$_{14}$P$_4$S$_2$): C, 55.98 (55.28%); H, 9.78 (9.71%); N, 2.00% (2.04%). The yield for [Eu(TBPO)$_4$(NO$_3$)$_2$]NTf$_2$ is 71%. *Anal.* Calc. (found) for [Eu(TBPO)$_4$ (NO$_3$)$_2$]NTf$_2$ (C$_{50}$H$_{108}$EuF$_6$N$_3$O$_{14}$P$_4$S$_2$): C, 42.01 (41.63%); H, 7.62 (7.47%); N, 2.94% (2.84%).

In order to obtain pure solid product, the white crude solid were dissolved into a mixed solvent of acetonitrile and water at volume ratio of 2:1, and the acetonitrile was volatilized very slowly. The obtained transparent rodlike crystal was then characterized by ESI-HRMS and single-crystal X-ray analysis. The structure of the crystal was proved to be [Eu(TPhPO)$_4$(NO$_3$)$_2$]NTf$_2$ by organic element analyses. The yield is 82%. *Anal.* Calc. (found) for [Eu(TPhPO)$_4$(NO$_3$)$_2$]NTf$_2$ (C$_{74}$H$_{60}$EuF$_6$N$_3$O$_{14}$P$_4$S$_2$): C, 53.24 (53.26%); H, 3.62 (3.79%); N, 2.52% (2.52%).

3. Results and discussion

3.1. The crystal structure of [Eu(TPhPO)$_4$(NO$_3$)$_2$]NTf$_2$

In order to ascertain how NTf$_2^-$ influences the structure, we synthesized the complex [Eu(TPhPO)$_4$(NO$_3$)$_2$]NTf$_2$ as mentioned above. The X-ray crystallographic data for the complex are shown in Table 2. Selected bond lengths and angles are listed in Table 3. The structure of the crystal [Eu(TPhPO)$_4$(NO$_3$)$_2$]NTf$_2$ is shown in Fig. 1, in which Eu^{3+} is coordinated by four TPhPO molecules and two bidentate nitrates. Four oxygen atoms of TPhPO are almost in a same plane, while two bidentate nitrates coordinate with Eu^{3+} oppositely. The average Eu–O(P) distance is 2.308(2) Å and the average Eu–O(N) distance is 2.491(2) Å for [Eu(TPhPO)$_4$(NO$_3$)$_2$]NTf$_2$. The geometry of the eight-coordinate complex [Eu(TPhPO)$_4$

Table 2
Crystallographic data for the complex [Eu(TPhPO)$_4$(NO$_3$)$_2$]NTf$_2$.

Empirical formula	C$_{74}$H$_{60}$N$_3$O$_{14}$P$_4$S$_2$EuF$_6$
Formula weight	1669.21
T (K)	180.00(10)
Crystal system	triclinic
Space group	$P\bar{1}$
a (Å)	12.4101(6)
b (Å)	18.0206(9)
c (Å)	19.6067(11)
α (°)	116.261(5)
β (°)	96.337(4)
γ (°)	100.051(4)
V (Å^3)	3783.5(4)
Z	2
ρ_{calc} (g/cm^3)	1.465
μ (mm^{-1})	1.047
$F(000)$	1692.0
Crystal size (mm^3)	0.1 × 0.1 × 0.05
Radiation (Å)	Mo Kα (λ = 0.71073)
2Θ range for data collection (°)	5.994 to 52.044
Index ranges	$-14 \leqslant h \leqslant 15$, $-17 \leqslant k \leqslant 22$, $-24 \leqslant l \leqslant 18$
Reflections collected	21502
Independent reflections	14397 [R_{int} = 0.0314, R_{sigma} = 0.0601]
Data/restraints/parameters	14397/40/1073
Goodness-of-fit (GOF) on F^2	1.086
Final R indexes [$I \geqslant 2\sigma$ (I)]	R_1 = 0.0386, wR_2 = 0.0814
Final R indexes [all data]	R_1 = 0.0500, wR_2 = 0.0912
Largest difference in peak and hole (e Å^{-3})	1.43/−1.28

Table 3
Selected bond lengths [Å] and angles [°] for [Eu(TPhPO)$_4$(NO$_3$)$_2$]NTf$_2$.

|			
Eu1–N1	2.913(3)	Eu1–O5	2.511(2)
Eu1–N2	2.903(3)	Eu1–O7	2.311(2)
Eu1–O1	2.481(2)	Eu1–O8	2.311(2)
Eu1–O2	2.510(2)	Eu1–O9	2.286(2)
Eu1–O4	2.461(2)	Eu1–O10	2.325(2)
N1–O1	1.264(3)	N2–O4	1.265(3)
N1–O2	1.272(4)	N2–O5	1.272(3)
N1–O3	1.215(4)	N2–O6	1.218(4)
O8–Eu1–O9	93.44(8)	O6–N2–Eu1	175.7(3)
O8–Eu1–O7	98.22(8)	O6–N2–O4	121.8(3)
O8–Eu1–O10	153.21(8)	O6–N2–O5	121.4(3)
O7–Eu1–O2	125.72(8)	P1–O7–Eu1	159.56(14)
O7–Eu1–O10	90.56(8)	P2–O8–Eu1	162.48(14)
O10–Eu1–O2	77.01(8)	P3–O9–Eu1	164.73(15)
		P4–O10–Eu1	166.58(14)
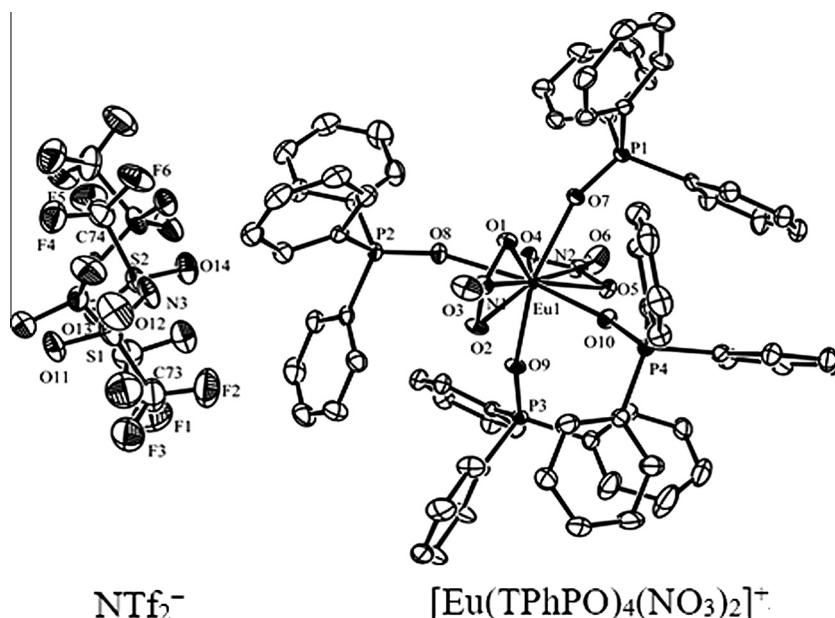
Fig. 1. The single crystal structures of the cation $[Eu(TPhPO)_4(NO_3)_2]^+$ and the anion NTf_2^- in the $[Eu(TPhPO)_4(NO_3)_2]NTf_2$ crystal.

$(NO_3)_2]NTf_2$ can be regarded as a trans pseudo-octahedral if the nitrates are considered as pseudo-monodentate ligands [6]. From the crystal data, it is noted that NTf_2^- is not coordinated with Eu^{3+}, but functions as a counter anion. The complex structure is significantly different from $Eu(TPhPO)_3(NO_3)_3 \cdot Me_2CO$ and $Eu(TPhPO)_2(NO_3)_3 \cdot ethanol$ which were formed in acetone and ethanol, respectively [5]. These two reported complexes are all nine-coordinate containing three bidentate nitrates. The structural difference is that $Eu(TPhPO)_3(NO_3)_3 \cdot Me_2CO$ contains three monodentate TPhPO and $Eu(TPhPO)_2(NO_3)_3 \cdot ethanol$ has two monodentate TPhPO and a monodentate ethanol. Other previous researches also showed that the reaction of TPhPO with lanthanide nitrates in ethanol or acetone produces $Ln(TPhPO)_3(NO_3)_3$ containing nine-coordinate metal centres based on three phosphine oxides and three bidentate nitrates [2,5,27]. With a sixfold excess of TPhPO in acetone, the reaction of $Ln(NO_3)_3 \cdot 6H_2O$ (Ln = La, Ce, Pr or Nd) with TPhPO in acetone resulted in the formation of $[Ln(TPhPO)_4(NO_3)_3] \cdot Me_2CO$. But for Sm, Eu or Gd, $Ln(TPhPO)_3(NO_3)_3$ were formed instead [6]. From the structure of $[Eu(TPhPO)_4(NO_3)_2]NTf_2$ obtained in this work, it can be found that the involvement of NTf_2^- induces the formation of the eight-coordinate $[Eu(TPhPO)_4(NO_3)_2]NTf_2$, with only a twofold molar excess of TPhPO in ethanol and water, rather than the nine-coordinate $Eu(TPhPO)_3(NO_3)_3$, whereas the tenfold molar excess of TPhPO to $Eu(NO_3)_3$ in ethanol or acetone causes the formation of $Eu(TPhPO)_3(NO_3)_3$ [6]. Therefore, $[Eu(TPhPO)_4(NO_3)_2]NTf_2$ is reported herein as a first eight-coordinate complex among the Eu-complexes with TPhPO in the presence of NTf_2^-.

3.2. High-resolution mass spectra

The $[Eu(TPhPO)_4(NO_3)_2]NTf_2$ crystal structure was further characterized through electrospray ionization high resolution mass spectra (ESI-HRMS). As shown in Fig. 2a, a peak in positive mode appears at m/z 1389.22187 that is attributed to $[Eu(TPhPO)_4(NO_3)_2]^+$. Peaks at m/z 1111.14550, 831.06491 and 663.62478 represent $[Eu(TPhPO)_3(NO_3)_2]^+$, $[Eu(TPhPO)_2(NO_3)_2]^+$ and $[Eu(TPhPO)(NO_3)_2]^+$, respectively.

The ESI-HRMS were also recorded on the CH_3CN solutions of $[Eu(TOPO)_4(NO_3)_2]NTf_2$ and $[Eu(TBPO)_4(NO_3)_2]NTf_2$. As shown in

Fig. 2b, the base peak at m/z 773.74246 in the positive ionization mode of $[Eu(TOPO)_4(NO_3)_2]NTf_2$ can be ascribed to $[2TOPO+H]^+$. Peaks displayed at m/z 1822.36612 and 1435.99438 in positive mode are attributable to $[Eu(TOPO)_4(NO_3)_2]^+$ and $[Eu(TOPO)_3(NO_3)_2]^+$, respectively. For $[Eu(TBPO)_4(NO_3)_2]NTf_2$, two main peaks corresponding to $[Eu(TBPO)_4(NO_3)_2]^+$ and $[Eu(TBPO)_3(NO_3)_2]^+$ can be found at m/z 1149.37669 and 931.44010 in Fig. 2c. The negative spectra of these three complexes are identical. The peak (m/z = 279.91791) in negative spectrum, representing NTf_2^- of $[Eu(TBPO)_4(NO_3)_2]NTf_2$, can be observed in Fig. 2d. The details of spectra assignments for the three complexes are listed in Table 4.

3.3. Infrared spectra

The infrared spectra (Fig. 3) of the three complexes contain some typical features of the phosphine oxide and nitrate. The peaks positions and assignments are compiled in Table 5. IR spectra results show the presence of bidentate nitrates (Scheme 2) in all the three Eu complexes. The symmetric stretching mode (v_1) of the $-NO_2$ group in the three complexes can be assigned at 1282 cm^{-1} (TOPO complex), 1288 cm^{-1} (TBPO complex) and 1284 cm^{-1} (TPhPO complex). Peaks of N–O stretching mode (v_2) appear at around 1026–1028 cm^{-1}. The asymmetric stretching mode (v_3) of the $-NO_2$ group is split for $[Eu(TOPO)_4(NO_3)_2]NTf_2$ (1468 and 1493 cm^{-1}) and $[Eu(TBPO)_4(NO_3)_2]NTf_2$ (1466 and 1495 cm^{-1}), whereas v_3 of $[Eu(TPhPO)_4(NO_3)_2]NTf_2$ remains a single band at 1477 cm^{-1}. The P–O stretches are observed at 1120 cm^{-1}, 1117 cm^{-1} and 1147 cm^{-1} for $[Eu(TOPO)_4(NO_3)_2]NTf_2$, $[Eu(TBPO)_4(NO_3)_2]NTf_2$ and $[Eu(TPhPO)_4(NO_3)_2]NTf_2$, respectively, which are at lower wavenumbers than the corresponding P–O stretches of the free ligands TOPO (1146 cm^{-1}), TBPO (1149 cm^{-1}) and TPhPO (1192 cm^{-1}). Other peaks wavenumbers like 1354 cm^{-1} and 1059 cm^{-1} are associated with the characteristics of NTf_2^- as compared with the IR spectra of $LiNTf_2$ and $C_4mimNTf_2$.

3.4. ^{31}P NMR spectra

Solution properties of the complexes were investigated in CH_2Cl_2 by ^{31}P NMR spectroscopy. The resonance at −100.48 ppm
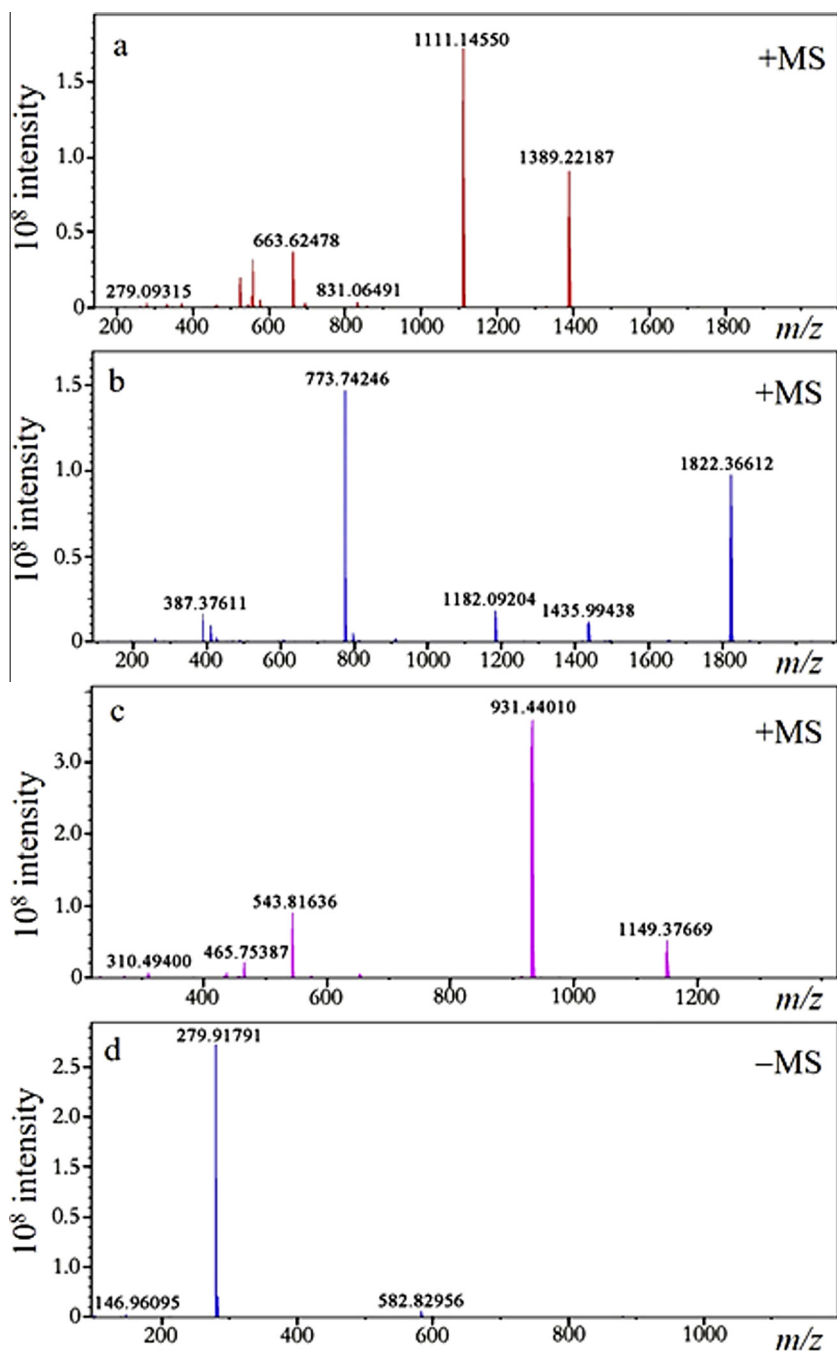
Fig. 2. Positive mode mass spectra of $[Eu(TPhPO)_4(NO_3)_2]NTf_2$ (a), $[Eu(TOPO)_4(NO_3)_2]NTf_2$ (b) and $[Eu(TBPO)_4(NO_3)_2]NTf_2$ (c). Negative mode mass spectrum of $[Eu(TBPO)_4(NO_3)_2]NTf_2$ (d).

Table 4
Compositions of the identified ions from the ESI-HRMS characterization of synthesized $[Eu(TPhPO)_4(NO_3)_2]NTf_2$, $[Eu(TOPO)_4(NO_3)_2]NTf_2$ and $[Eu(TBPO)_4(NO_3)_2]NTf_2$.

Complexes	m/z	Relative intensity (%)	Composition
$[Eu(TPhPO)_4(NO_3)_2]NTf_2$	1389.22187	51	$[Eu(TPhPO)_4(NO_3)_2]^+$
	1111.14550	100	$[Eu(TPhPO)_3(NO_3)_2]^+$
	831.06491	3	$[Eu(TPhPO)_2(NO_3)_2]^+$
$[Eu(TOPO)_4(NO_3)_2]NTf_2$	1822.36612	67	$[Eu(TOPO)_4(NO_3)_2]^+$
	1435.99438	7	$[Eu(TOPO)_3(NO_3)_2]^+$
	773.74246	100	$2TOPO+H^+$
	387.37611	10	$TOPO+H^+$
$[Eu(TBPO)_4(NO_3)_2]NTf_2$	1149.37669	16	$[Eu(TBPO)_4(NO_3)_2]^+$
	931.44010	100	$[Eu(TBPO)_3(NO_3)_2]^+$
	279.91719	100	NTf_2^-

The m/z values of the Eu-species mainly correspond to those for 153-Eu isotope.
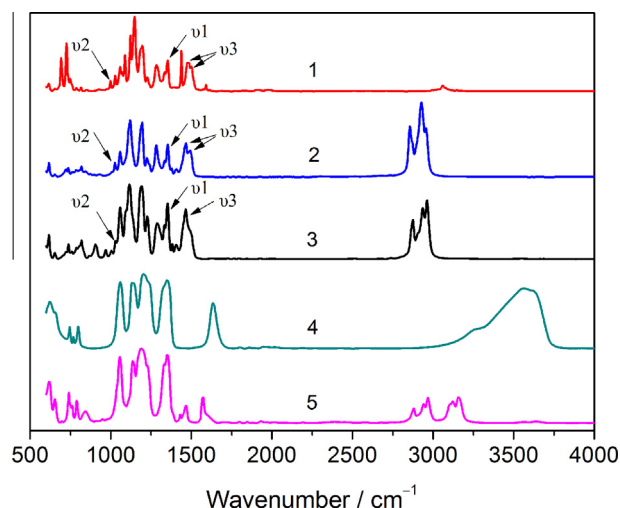
Fig. 3. IR spectra of [Eu(TPhPO)$_4$(NO$_3$)$_2$]NTf$_2$ (1), [Eu(TOPO)$_4$(NO$_3$)$_2$]NTf$_2$ (2), [Eu(TBPO)$_4$(NO$_3$)$_2$]NTf$_2$ (3), LiNTf$_2$ (4) and C$_4$mimNTf$_2$ (5).

of [Eu(TPhPO)$_4$(NO$_3$)$_2$]NTf$_2$ represents the P resonance of cation [Eu(TPhPO)$_4$(NO$_3$)$_2$]$^+$ in solution (see Fig. 4a). The result confirms a assumption proposed by Levason et al. [6] concerning the existence of a tetrakis(phosphine oxide) complex with a weak resonance at −101 ppm on the addition of a tenfold molar excess of TPhPO to Eu(TPhPO)$_3$(NO$_3$)$_3$. By adding NTf$_2$, we successfully prepared the tetrakis(phosphine oxide) complex of Eu^{3+} that had not be obtained actually by Levason et al. The spectra of the [Eu(TBPO)$_4$(NO$_3$)$_2$]NTf$_2$ and [Eu(TOPO)$_4$(NO$_3$)$_2$]NTf$_2$ are similar. The ^{31}P NMR spectrum of [Eu(TBPO)$_4$(NO$_3$)$_2$]NTf$_2$ in CH$_2$Cl$_2$ at

ambient temperature exhibits a single peak at −42.20 ppm (Fig. 4c), which can be assigned to the P resonance of cation species [Eu(TBPO)$_4$(NO$_3$)$_2$]$^+$. The P chemical shift of [Eu(TBPO)$_4$(NO$_3$)$_2$]$^+$ (−42.20 ppm) is higher than that of Eu(NO$_3$)$_3$(Et$_3$PO)$_3$ (−60.5 ppm) [7], Eu(NO$_3$)$_3$(iBu$_3$PO)$_3$ (−52.3 ppm), [9] Eu(NO$_3$)$_3$(tBu$_3$PO)$_2$ (−57.7 ppm) [10] and Eu(NO$_3$)$_3$(iPr$_3$PO)$_n$ (−68.6 ppm) [28] because of more ligands in the complex [Eu(TBPO)$_4$(NO$_3$)$_2$] NTf$_2$. A single signal at −39.93 ppm (Fig. 4b) was also observed at room temperature for [Eu(TOPO)$_4$(NO$_3$)$_2$]NTf$_2$ but narrower than [Eu(TBPO)$_4$(NO$_3$)$_2$]NTf$_2$, which indicated a slower ligand exchange of [Eu(TOPO)$_4$(NO$_3$)$_2$]NTf$_2$ in CH$_2$Cl$_2$. Both the broaden peak and low chemical shift of [Eu(TBPO)$_4$(NO$_3$)$_2$]NTf$_2$ can be explained by the low basicity of TBPO compared with that of TOPO in [Eu(TOPO)$_4$(NO$_3$)$_2$]NTf$_2$. There is no ^{31}P signal evidence of free ligands in solutions suggesting no dissociation of these complexes.

3.5. Thermogravimetric analyses

In order to assess the thermal stabilities and the phase behaviors of these complexes, the decomposition temperatures were determined using TGA. The three complexes possess good thermal stability up to 250 °C due to the absence of phosphine oxide and nitrate ligands (Fig. 5). The complex [Eu(TOPO)$_4$(NO$_3$)$_2$]NTf$_2$ was decomposed in two degradation steps. The initial weight loss of 78.5% (calcd 79.4%) in the temperature range 250–390 °C was assigned to the decomposition of four TOPO molecules and two nitrate anions per formula unit. The second step from 390 °C to 550 °C with a weight loss of 12.4% (calcd 13.3%), which corresponds to the decomposition of NTf$_2^-$. The TGA curves of [Eu(TBPO)$_4$(NO$_3$)$_2$]NTf$_2$ and [Eu(TPhPO)$_4$(NO$_3$)$_2$]NTf$_2$ showed similar one-step weight loss profiles. In the temperature range

Table 5
Infrared positions and assignments for [Eu(TOPO)$_4$(NO$_3$)$_2$]NTf$_2$, [Eu(TBPO)$_4$(NO$_3$)$_2$]NTf$_2$ and [Eu(TPhPO)$_4$(NO$_3$)$_2$]NTf$_2$.

Complex	v_{PO} (cm^{-1})*	v_3 (cm^{-1})	v_1 (cm^{-1})	v_2 (cm^{-1})	v_4 (cm^{-1})	v_5 (cm^{-1})
[Eu(TOPO)$_4$(NO$_3$)$_2$]NTf$_2$	1120	1468, 1493	1282	1026	818	737
[Eu(TBPO)$_4$(NO$_3$)$_2$]NTf$_2$	1117	1466, 1495	1288	1028	820	739
[Eu(TPhPO)$_4$(NO$_3$)$_2$]NTf$_2$	1147	1477	1284	1028	816	748

* P–O stretches of the free ligands TOPO, TBPO and TPhPO are 1146 cm^{-1}, 1149 cm^{-1} and 1192 cm^{-1}, respectively.
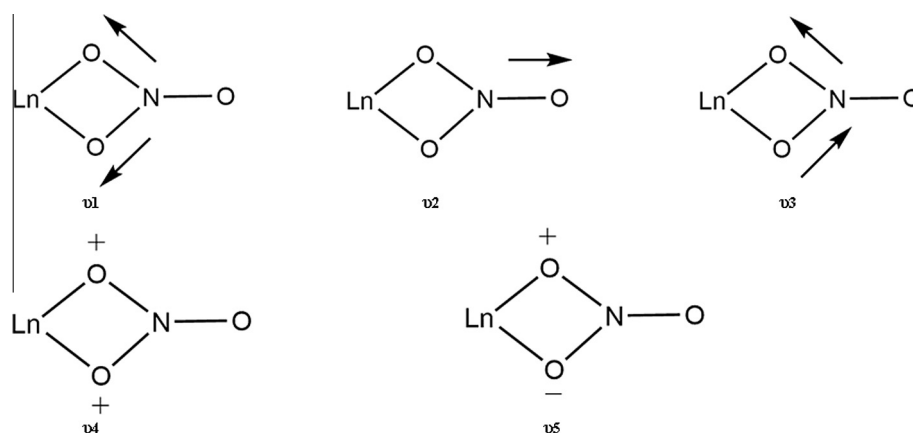
v_1: symmetric stretching mode of the –NO$_2$ group
v_2: N-O stretching mode
v_3: asymmetric stretching mode of the –NO$_2$ group
v_4 and v_5: non planar rocking frequency modes

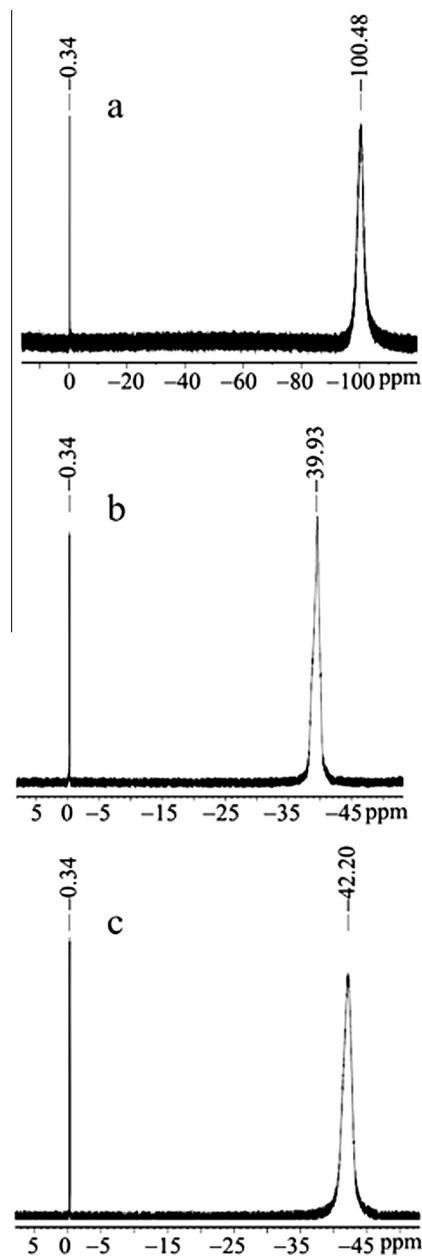**Scheme 2.** Stretching modes of NO$_3^-$ in complexes.

Fig. 4. ^{31}PNMR spectra of [Eu(TPhPO)$_4$(NO$_3$)$_2$]NTf$_2$ (a), [Eu(TOPO)$_4$(NO$_3$)$_2$]NTf$_2$ (b) and [Eu(TBPO)$_4$(NO$_3$)$_2$]NTf$_2$ (c) in CH$_2$Cl$_2$ (the peak around zero represents the P chemical shift of external standard H$_3$PO$_4$).

Fig. 5. TGA curves of [Eu(TPhPO)$_4$(NO$_3$)$_2$]NTf$_2$ (1), [Eu(TOPO)$_4$(NO$_3$)$_2$]NTf$_2$ (2), [Eu(TBPO)$_4$(NO$_3$)$_2$]NTf$_2$ (3), TPhPO (4), and LiNTf$_2$ (5).
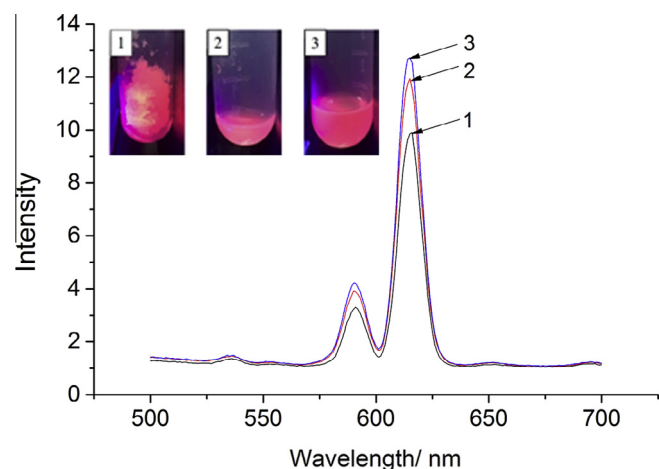
Fig. 6. Emission spectra of 1 mmol dm^{-3} [Eu(TPhPO)$_4$(NO$_3$)$_2$]NTf$_2$ (1), [Eu(TBPO)$_4$(NO$_3$)$_2$]NTf$_2$ (2) and [Eu(TOPO)$_4$(NO$_3$)$_2$]NTf$_2$ (3) in acetonitrile at room temperature. The three emission spectra were normalized in order to compare the relative intensity of all emission peaks (upper left conner). Inset: the three compounds under UV radiation.

250–500 °C, the two compounds rapidly decomposed to their respective europium oxide. The TGA profiles of Ln(TPhPO)$_2$(phen)(NO$_3$)$_3$ (phen = 1,10-phenanthroline, Ln = Ce, Gd, Tb, Ho, Eu) been synthesized by Xu et al. also show similar one-step weight loss (no optimal result of Eu(TPhPO)$_2$(phen)(NO$_3$)$_3$ could be obtained) [29]. We think that the thermal decomposition properties of these compounds possess certain similarities.

3.6. Emission spectra

The emission spectra of the three complexes in acetonitrile show the characteristic transitions for Eu^{3+} ions. From Fig. 6, it can be found that the emission spectra of [Eu(TOPO)$_4$(NO$_3$)$_2$]NTf$_2$, [Eu(TBPO)$_4$(NO$_3$)$_2$]NTf$_2$ and [Eu(TPhPO)$_4$(NO$_3$)$_2$]NTf$_2$ are almost the same and that all $^5D_0 \rightarrow {}^7F_J$ (J = 0–4) transitions are observed. The emission spectra on excitation at 395 nm show four main
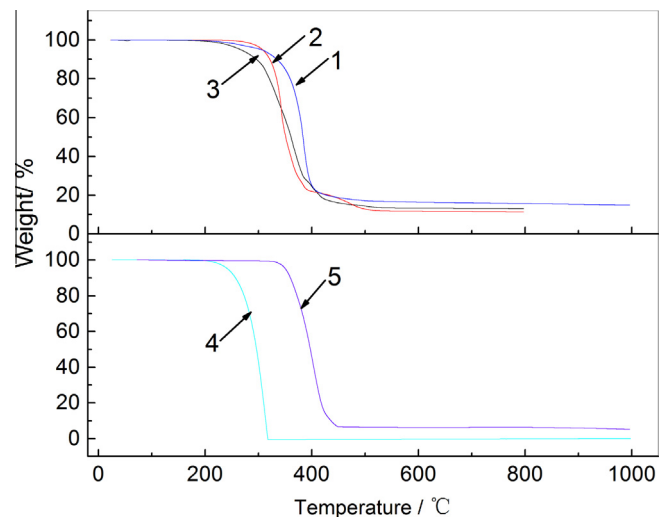
bands at 590, 616, 651 and 696 nm. The sharp and narrow emission band at 616 nm is characteristic of the hypersensitive $^5D_0 \rightarrow {}^7F_2$ transition of Eu, which is the most intensive emission among these peaks. The peaks at about 651 nm and 696 nm are due to the transition of $^5D_0 \rightarrow {}^7F_3$ and $^5D_0 \rightarrow {}^7F_4$. The relative intensities of these emission peaks in the three complexes are identical, which indicates that the metal ions in [Eu(TOPO)$_4$(NO$_3$)$_2$]NTf$_2$, [Eu(TBPO)$_4$(NO$_3$)$_2$]NTf$_2$ and [Eu(TPhPO)$_4$(NO$_3$)$_2$]NTf$_2$ have similar coordination environments. The two Eu-containing ionic liquids show intense red photoluminescence (see the inset in Fig. 6) when irradiated with UV radiation, which may have potential optional applications as soft materials.

Considering the similar IR and fluorescence spectra among TOPO, TBPO and TPhPO complexes, we assume that coordination structures of [Eu(TOPO)$_4$(NO$_3$)$_2$]NTf$_2$ and [Eu(TBPO)$_4$(NO$_3$)$_2$]NTf$_2$ are similar to that of [Eu(TPhPO)$_4$(NO$_3$)$_2$]NTf$_2$. Both [Eu(TOPO)$_4$(NO$_3$)$_2$]NTf$_2$ and [Eu(TBPO)$_4$(NO$_3$)$_2$]NTf$_2$ have two bidentate nitrates and four monodentate ligands. In the structures of [Eu(TOPO)$_4$(NO$_3$)$_2$]NTf$_2$ and [Eu(TBPO)$_4$(NO$_3$)$_2$]NTf$_2$ twelve alkyl chains exist. Besides, no hydrogen-bonding network or water

molecules were found in $[Eu(TOPO)_4(NO_3)_2]NTf_2$ and $[Eu(TBPO)_4(NO_3)_2]NTf_2$. This structure can further decrease the interaction between the ions. $[Eu(TOPO)_4(NO_3)_2]NTf_2$ and $[Eu(TBPO)_4(NO_3)_2]NTf_2$ cannot be stacked up easily compared with $[Eu(TPhPO)_4(NO_3)_2]NTf_2$. Therefore, they do not crystalize at room temperature, whereas $[Eu(TPhPO)_4(NO_3)_2]NTf_2$ exists in solid state. A relatively high melting point, i.e. 253 °C, of $[Eu(TPhPO)_4(NO_3)_2]NTf_2$ was measured in this work. The structures of $[Eu(TOPO)_4(NO_3)_2]NTf_2$ and $[Eu(TBPO)_4(NO_3)_2]NTf_2$ are significantly different from the common europium nitrates complexes $Eu(TRPO)_3(NO_3)_3$ (R = butyl, octyl) [1,2]. Lanthanide nitrate complexes with TRPO (R = ethyl, [7] cyclohexyl, [8] isobutyl [9]) in some recent researches also indicate that the structure for these complexes is $Ln(TRPO)_3(NO_3)_3$. The involvement of NTf_2^- shows that the formation of NTf_2^--based complexes ($[Eu(TOPO)_4(NO_3)_2]NTf_2$ and $[Eu(TBPO)_4(NO_3)_2]NTf_2$) are preferred to that of $Ln(TRPO)_3(NO_3)_3$. These complexes are constituted by electrostatic interactions between the NTf_2^- and $[Eu(TRPO)_4(NO_3)_2]^+$. This interaction between Eu^{3+} and NTf_2^- is weak, which is similar to that between UO_2^{2+} and NTf_2^- in our previous work [30]. However, the result is different from that of the single crystal structure $[CsBPC_6]NTf_2$ (BPC_6: bis(2-propyloxy)calix [4]crown-6) in our another published work, in which NTf_2^- takes part in the coordination with Cs^+ [31].

In recent years, metal-containing ionic liquids have received much attention as new promising soft materials which combine the properties of ionic liquids with other intrinsic properties (such as luminescent, magnetic, or catalytic properties) based on the incorporated metals [32–39]. Several lanthanide-containing ILs have been reported concerning their luminescent properties. Ionic liquids $[C_4mim]_{x-3}[Ln(NCS)_x(H_2O)_y]$ ($x = 6–8$, $y = 0–2$) [32] are transparent liquids at room temperature, which are candidates for catalytic and spectroscopic applications. Some other Eu-containing ionic liquids incorporating NTf_2^- ($[C_4mim][Eu(NTf_2)_4]$ and $[C_4mpyr]_2[Eu(NTf_2)_5]$) were reported to overcome the obstacle of the energy absorbing by containing water [34]. Tao et al. synthesized some water-free lanthanum ionic liquids $[C_nmim]_3[La(NO_3)_6]$, which are thermal and moisture stable [38]. Other NTf_2^--based metal-containing ionic liquids were also reported, like $[Fe(C_5Me_4C_nH_{2n+1})(C_5Me_4H)]NTf_2$, [40] $[Cu(acac)(BuMe_3en)]NTf_2$ [41] and so on. Lanthanide-containing ionic liquids constituted by both organophosphorous ligands and NTf_2^- were less reported. The Eu-containing ionic liquids $[Eu(TOPO)_4(NO_3)_2]NTf_2$ and $[Eu(TBPO)_4(NO_3)_2]NTf_2$ in this work can also help understand the possible extraction species in the $C_nmimNTf_2$-based extraction system. For most neutral extractants, the extraction mechanism is often cation-exchange mechanism in ILs. Therefore, based on the complexes reported in this work, we suggest that a possible extraction mechanism that the cation species $[Eu(TRPO)_4(NO_3)_2]^+$ may exchange with C_nmim^+, leading to the formation of $[Eu(TRPO)_4(NO_3)_2]NTf_2$ with NTf_2^- in the ILs $C_nmimNTf_2$. Further work will be reported elsewhere.

4. Conclusions

In the present study, complexes $[Eu(TOPO)_4(NO_3)_2]NTf_2$, $[Eu(TBPO)_4(NO_3)_2]NTf_2$ and $[Eu(TPhPO)_4(NO_3)_2]NTf_2$ were synthesized and characterized by organic element analyses and ESI-HRMS. $[Eu(TOPO)_4(NO_3)_2]NTf_2$ and $[Eu(TBPO)_4(NO_3)_2]NTf_2$ are Eu-containing ionic liquids at room temperature, in which organophosphorous complexes of Eu^{3+} constitute the cations and NTf_2^- acts as counter anion. The crystal structure of $[Eu(TPhPO)_4(NO_3)_2]NTf_2$ shows that an Eu^{3+} cation is coordinated by four TPhPO and two bidentate nitrates. The four oxygen atoms of TPhPO are almost in the same plane and two bidentate nitrates coordinate with Eu^{3+} oppositely. NTf_2^- is not coordinated with Eu^{3+} and

functions as the counter anion instead. The complex is the first tetra-TPhPO complex constituted by $Eu(NO_3)_3$ and TPhPO. The ^{31}P NMR spectra of $[Eu(TOPO)_4(NO_3)_2]NTf_2$ and $[Eu(TBPO)_4(NO_3)_2]NTf_2$ in CH_2Cl_2 at ambient temperature exhibit a single peak, which can be assigned to the P resonance of cation species $[Eu(TRPO)_4(NO_3)_2]^+$. Thermogravimetric analysis (TGA) measurements and luminescence emissions illustrate the similar properties among $[Eu(TOPO)_4(NO_3)_2]NTf_2$, $[Eu(TBPO)_4(NO_3)_2]NTf_2$ and $[Eu(TPhPO)_4(NO_3)_2]NTf_2$. The structural difference between $[Eu(TOPO)_4(NO_3)_2]NTf_2$ and $Eu(TOPO)_3(NO_3)_3$ can help understand the fact that new extraction species may exist in the NTf_2^--based ILs extraction systems compared with the normal organic solvent extraction systems.

Acknowledgments

Appendix A. Supplementary data

CCDC 986604 contains the supplementary crystallographic data for $[Eu(TPhPO)_4(NO_3)_2]NTf_2$. These data can be obtained free of charge via http://www.ccdc.cam.ac.uk/conts/retrieving.html, or from the Cambridge Crystallographic Data Centre, 12 Union Road, Cambridge CB2 1EZ, UK; fax: (+44) 1223-336-033; or e-mail: deposit@ccdc.cam.ac.uk.

References

[1] V.K. Manchanda, K. Chander, N.P. Singh, G.M. Nair, J. Inorg. Nucl. Chem. 39 (1977) 1039.
[2] A.M.G. Massabni, M.L.R. Gibran, O.A. Serra, Inorg. Nucl. Chem. Lett. 14 (1978) 419.
[3] J. Goffart, G. Duyckaer, Anal. Chim. Acta 46 (1969) 91.
[4] D.R. Cousins, F.A. Hart, J. Inorg. Nucl. Chem. 29 (1967) 1745.
[5] G. Valle, G. Casotto, P.L. Zanonato, B. Zarli, Polyhedron 5 (1986) 2093.
[6] W. Levason, E.H. Newman, M. Webster, Polyhedron 19 (2000) 2697.
[7] A. Bowden, K. Singh, A.W.G. Platt, Polyhedron 42 (2012) 30.
[8] A.P. Hunter, A.M.J. Lees, A.W.G. Platt, Polyhedron 26 (2007) 4865.
[9] A. Bowden, P.N. Horton, A.W.G. Platt, Inorg. Chem. 50 (2011) 2553.
[10] A. Bowden, S.J. Coles, M.B. Pitak, A.W.G. Platt, Inorg. Chem. 51 (2012) 4379.
[11] J. Dupont, R.F. de Souza, P.A.Z. Suarez, Chem. Rev. 102 (2002) 3667.
[12] T. Welton, Coord. Chem. Rev. 248 (2004) 2459.
[13] X.Q. Sun, H.M. Luo, S. Dai, Chem. Rev. 112 (2012) 2100.
[14] K. Shimojo, K. Kurahashi, H. Naganawa, Dalton Trans. (2008) 5083.
[15] M.L. Dietz, D.C. Stepinski, Green Chem. 7 (2005) 747.
[16] A.E. Visser, M.P. Jensen, I. Laszak, K.L. Nash, G.R. Choppin, R.D. Rogers, Inorg. Chem. 42 (2003) 2197.
[17] M.L. Dietz, J.A. Dzielawa, Chem. Commun. 20 (2001) 2124.
[18] M.P. Jensen, J.A. Dzielawa, P. Rickert, M.L. Dietz, J. Am. Chem. Soc. 124 (2002) 10664.
[19] M.P. Jensen, J. Neuefeind, J.V. Beitz, S. Skanthakumar, L. Soderholm, J. Am. Chem. Soc. 125 (2003) 15466.
[20] V.A. Cocalia, M.P. Jensen, J.D. Holbrey, S.K. Spear, D.C. Stepinski, R.D. Rogers, Dalton Trans. (2005) 1966.
[21] A. Rout, S. Karmakar, K.A. Venkatesan, T.G. Srinivasan, P.R.V. Rao, Sep. Purif. Technol. 81 (2011) 109.
[22] A. Rout, K.A. Venkatesan, T.G. Srinivasan, P.R.V. Rao, Sep. Purif. Technol. 76 (2011) 238.
[23] K. Binnemans, Chem. Rev. 105 (2005) 4148.
[24] K. Nakashima, F. Kubota, T. Maruyama, M. Goto, Ind. Eng. Chem. Res. 44 (2005) 4368.
[25] X.Q. Sun, D.B. Wu, J. Chen, D.Q. Li, J. Chem. Technol. Biotechnol. 82 (2007) 267.
[26] P. Bonhote, A.P. Dias, N. Papageorgiou, K. Kalyanasundaram, M. Gratzel, Inorg. Chem. 35 (1996) 1168.
[27] D.R. Cousins, F.A. Hart, J. Inorg. Nucl. Chem. 29 (1967) 2965.
[28] A. Bowden, S.J. Coles, M.B. Pitak, A.W.G. Platt, Polyhedron 68 (2014) 258.
[29] H.F. Li, B. Zheng, K.W. Huang, Coord. Chem. Rev 116 (2015) 293.
[30] S. Gao, T.X. Sun, Q.D. Chen, X.H. Shen, J. Hazard. Mater. 263 (2013) 562.

[31] T.X. Sun, Z.M. Wang, X.H. Shen, Inorg. Chim. Acta 390 (2012) 8.
[32] P. Nockemann, B. Thijs, N. Postelmans, K. Van Hecke, L. Van Meervelt, K. Binnemans, J. Am. Chem. Soc. 128 (2006) 13658.
[33] B. Mallick, B. Balke, C. Felser, A.-V. Mudring, Angew. Chem., Int. Ed. 47 (2008) 7635.
[34] S. Tang, A. Babai, A.V. Mudring, Angew. Chem., Int. Ed. 47 (2008) 7631.
[35] G.H. Tao, Y.G. Huang, J.A. Boatz, J.n.M. Shreeve, Chem. Eur. J. 14 (2008) 11167.
[36] H.R. Li, P. Liu, H.F. Shao, Y.G. Wang, Y.X. Zheng, Z. Sun, Y.H. Chen, J. Mater. Chem. 19 (2009) 5533.
[37] A.S.R. Chesman, M. Yang, B. Mallick, T.M. Ross, I.A. Gass, G.B. Deacon, S.R. Batten, A.V. Mudring, Chem. Commun. 48 (2012) 124.
[38] S.P. Ji, M. Tang, L. He, G.H. Tao, Chem.-Eur. J. 19 (2013) 4452.
[39] T. Ohaion, Y. Kalisky, Y. Ben-Eliyahu, J.Y. Becker, A. Bettelheim, Eur. J. Inorg. Chem. 2013 (2013) 3477.
[40] Y. Funasako, T. Inagaki, T. Mochida, T. Sakurai, H. Ohta, K. Furukawa, T. Nakamura, Dalton Trans. 42 (2013) 8317.
[41] Y. Funasako, T. Mochida, K. Takahashi, T. Sakurai, H. Ohta, Chem.-Eur. J. 18 (2012) 11929.